



# CHORUS

This is the accepted manuscript made available via CHORUS. The article has been published as:

## Equation of state and high-pressure/high-temperature phase diagram of magnesium

G. W. Stinton, S. G. MacLeod, H. Cynn, D. Errandonea, W. J. Evans, J. E. Proctor, Y. Meng, and M. I. McMahon

Phys. Rev. B **90**, 134105 — Published 20 October 2014

DOI: [10.1103/PhysRevB.90.134105](https://doi.org/10.1103/PhysRevB.90.134105)

# Equation of State and High-Pressure High-Temperature Phase Diagram of Magnesium

G. W. Stinton,<sup>1</sup> S. G. MacLeod,<sup>2,3,4</sup> H. Cynn,<sup>5</sup> D. Errandonea,<sup>6</sup>  
W. J. Evans,<sup>5</sup> J. E. Proctor,<sup>1</sup> Y. Meng,<sup>7</sup> and M. I. McMahon<sup>1,4</sup>

<sup>1</sup>*SUPA, School of Physics and Astronomy,  
and Centre for Science at Extreme Conditions,  
The University of Edinburgh, EH9 3JZ, UK*

<sup>2</sup>*Atomic Weapons Establishment, Aldermaston, Reading, RG7 4PR, UK*

<sup>3</sup>*Institute of Shock Physics, Imperial College London, SW7 2AZ, UK*

<sup>4</sup>*Research Complex at Harwell, Didcot, Oxon, OX11 0FA, UK*

<sup>5</sup>*Lawrence Livermore National Laboratory,  
Condensed Matter and Material Division,  
Physics and Life Sciences Directorate, Livermore, CA 94551 USA*

<sup>6</sup>*Departamento de Física Aplicada - ICMUV,  
Universitat de Valencia, C/Dr. Moliner 50,  
Burjassot, E-46100, Valencia, Spain*

<sup>7</sup>*High Pressure Collaborative Access Team, Geophysical Laboratory,  
Carnegie Institution of Washington, Argonne, IL 60439, USA*

(Dated: August 28, 2014)

## Abstract

The phase diagram of magnesium has been investigated to 211 GPa at 300 K, and to 105 GPa at 4500 K, using a combination of x-ray diffraction and resistive and laser heating. The ambient pressure hcp structure is found to start transforming to the bcc structure at  $\sim 45$  GPa, with a large region of phase-coexistence that becomes smaller at higher temperatures. The bcc phase is stable to the highest pressures reached. The hcp-bcc phase boundary has been studied on both compression and decompression, and its slope is found to be negative, and steeper than calculations have previously predicted. The laser heating studies extend the melting curve of magnesium to 105 GPa, and suggest that at the highest pressures, the melting temperature increases more rapidly with pressure than previously reported. Finally, we observe some evidence of a new phase in the region of 10 GPa and 1200 K, where previous studies have reported a double-hexagonal close-packed (dhcp) phase. However, the additional diffraction peaks we observe cannot be accounted for by the dhcp phase alone.

## INTRODUCTION

Magnesium (Mg) has been described as a nearly free-electron metal up to pressures of around 100 GPa.<sup>1</sup> This, combined with interest in the pressure-driven transfer of electrons from the *sp*-band to the *3d*-band as the energy gap between the two decreases, has led to a number of theoretical studies<sup>2-9</sup> up to 30 TPa. Experimental studies have been conducted at room temperature (RT) to only the relatively modest pressure of 158 GPa.<sup>10</sup>

On compression, Mg transforms from the ambient-pressure hexagonal close-packed (hcp) phase to the body-centred cubic (bcc) phase between 44 and 58 GPa, with a large region of phase co-existence.<sup>11</sup> The bcc phase is known to be stable to 158 GPa.<sup>10</sup> At higher pressures, there have been several computational predictions of transformations to a number of different phases, including face-centred cubic<sup>5,8,12,13</sup>, simple cubic<sup>3</sup>, simple hexagonal<sup>8,13</sup>, simple cubic<sup>8</sup> and orthorhombic<sup>8</sup>. None of these post-bcc phases has been observed experimentally.

Kennedy and Newton<sup>14</sup> and Errandonea<sup>15</sup> determined the melting curve of hcp-Mg by resistivity measurements up to 12 GPa. Laser-heating experiments conducted by Errandonea *et al.*<sup>16</sup> agree with these measurements and reported that the melting temperature ( $T_m$ ) of Mg increases at around 45 K/GPa until 40 GPa<sup>17</sup> at which point  $dT_m/dP$  decreases such that by 70 GPa the melting temperature is almost pressure independent. There have been a number of *ab initio* calculations performed to determine the nature of the hcp-bcc phase boundary,<sup>2,4,6,13</sup> and these all show a negative slope, with the liquid-bcc-hcp triple point calculated to lie between 4 GPa and 1200 K<sup>2</sup> and 20 GPa and 1750 K.<sup>13</sup> Shock-compression studies along the Hugoniot<sup>18</sup> suggested the existence of a phase transition at 26.2(1.3) GPa and 900 K, which correlates well with the hcp-bcc phase boundary calculated by Moriarty and Althoff.<sup>4</sup>

In their high-temperature diffraction study to 18.6 GPa and 1527 K, Errandonea *et al.*<sup>19</sup> reported peak splittings and the appearance of new diffraction peaks which they interpreted as arising from a double-hexagonal close-packed (dhcp) phase that was recoverable back to RT at 8.05 GPa. However, a similar study by Cynn *et al.* to 25 GPa and 1900 K<sup>20</sup> saw no evidence of this dhcp phase. Metadynamics calculations<sup>9</sup> have addressed the relative stabilities of the hcp, dhcp and bcc phases, and while they found no stability range for the dhcp phase at RT, structural transformations back and forth between the hcp, dhcp, and bcc structures were found, but at 15 GPa and 500 K. These structural fluctuations were

reported to be driven by kinetics, and the authors suggest that the experimental observation of the dhcp structure at  $\sim 15$  GPa is because it is much more energetically favourable than the bcc structure at this pressure.<sup>9</sup>

Despite much previous study there still remain a number of inconsistencies between the observed and calculated behaviour of Mg. To address and resolve these, and to more fully explore the phase diagram of Mg, including the existence of the dhcp phase, we have made a series of x-ray diffraction studies using diamond anvil cells and different heating techniques up to 211 GPa at RT, and to  $\sim 4500$  K at 100 GPa.

## EXPERIMENTAL DETAILS

Different pressure cells and sample loadings were used in the three different types of experiment performed. For the RT compression experiments to 211 GPa, a Boehler-Almax<sup>21</sup> type diamond anvil cell (DAC), henceforth referred to as cell 1, equipped with bevelled diamonds and a rhenium gasket, was loaded with Mg powder of 99.999% purity purchased from Aldrich Chemicals. No pressure transmitting medium (PTM) was used. Powder angle-dispersive x-ray diffraction (ADXRD) data were collected on compression using the 16IDB HPCAT (High Pressure Collaborative Access Team) beamline at the Advanced Photon Source (APS), Argonne National Laboratory, Chicago, USA, using a wavelength of  $0.398 \text{ \AA}$  and an x-ray beamsize of  $5 \mu\text{m}$  in diameter. Cell 1 was loaded with micron-sized pieces of both copper (Cu) and tantalum (Ta) as pressure markers and data were collected to 211 GPa. Unfortunately, at this pressure, the anvils failed, terminating the experiment.

For the resistive heating studies we used six gas-membrane driven diamond anvil cells<sup>22</sup> equipped with diamonds with either  $250$  and  $300 \mu\text{m}$  culets and loaded with the same Mg powder as described above. Cu powder was used as the pressure marker, and no pressure transmitting medium was used so as to prevent chemical reactions at high temperatures. The cells were contained within a custom-designed vacuum vessel and were heated with external resistance heaters. The temperature was measured using a K-type thermocouple attached to one of the diamond anvils, close to the gasket. The diffraction data were collected on the I15 beamline at the Diamond Light Source using an incident x-ray wavelength of  $0.414 \text{ \AA}$ .

For the laser-heating measurements, pieces of  $8 \mu\text{m}$ -thick Mg foil (99.999% purity, Aldrich Chemicals) were loaded between insulating layers of approximately the same thickness of

MgO, into 12 Boehler-Almax cells equipped with diamonds with culet diameters ranging between 150 and 300  $\mu\text{m}$ . Cu powder was included with the sample as a pressure marker, but sample pressures were determined from the equation of state of MgO as it was present in every diffraction image. Simultaneous laser-heating and x-ray diffraction was carried out at 16IDB, HPCAT using an x-ray wavelength of 0.620  $\text{\AA}$  and a beam diameter (FWHM) of 5  $\mu\text{m}$ . Double-sided heating of the sample was achieved using two 100 W YLF fiber lasers and temperatures were measured separately from both sides with an imaging spectrograph<sup>23</sup>. The laser heating spot size was approximately 20  $\mu\text{m}$  (flat top area), significantly larger than the x-ray beam size. With the mirror pinhole setup,<sup>24</sup> the alignment of heating, temperature measurement and ADXRD spots can be directly monitored to ensure meaningful measurement results.

In all three sets of experiments, the 2-dimensional diffraction patterns were collected on either a MAR CCD (for laser heating at HPCAT) or a MAR345 image plate (resistive heating at HPCAT, and all studies at I15) and integrated azimuthally using Fit2d.<sup>25</sup> The resulting 1-dimensional diffraction profiles were analysed by LeBail fitting<sup>26</sup> of the whole profiles using the TOPAS Academic package,<sup>27</sup> or by analysis and least-squares fitting of the  $d$ -spacings of individual diffraction peaks.

The pressure of cell 1, and that of the DACs used in the resistive heating experiments, were determined from the Cu pressure marker in the sample chamber using the high-temperature Cu EoS of Cynn.<sup>28</sup> Because no pressure medium was utilised in these cells, the samples may therefore have experienced non-hydrostatic pressure conditions, leading to an overestimate of the measured volume of both the Mg sample and the Cu pressure marker,<sup>29</sup> and therefore an underestimate of the sample pressure. Because Mg is a soft metal, we expected any such effects to be small, but to quantify them we repeated the analysis of Singh and Takemura.<sup>29,30</sup> In the Cu pressure marker, there was no systematic effect below  $\sim 75$  GPa. At 100 GPa there was a small systematic overestimate of the Cu volume, leading to a pressure underestimate of 1 GPa, and this increased to 4 GPa at pressures above 200 GPa. All sample pressures were corrected for the effects of non-hydrostatic pressure conditions. The Mg thus acted as a good hydrostatic medium for the Cu pressure marker, and, as a result, there was no evidence for any non-hydrostatic pressure conditions within the hcp phase of Mg below 50 GPa. For the high-pressure bcc phase above 50 GPa, the Mg sample volume was found to be slightly overestimated at pressures above 100 GPa, and the sample volumes were corrected

accordingly.

Very few of the laser-heating diffraction images contained diffraction peaks from the Cu pressure marker, due to the small beam size and the need to position the laser and x-ray beam in places where good laser coupling could be achieved. Therefore, the MgO thermal insulation in the pressure chamber was used as the pressure calibrant. The pressures were determined using the thermal-EoS of Speziale *et al.*<sup>31</sup> The temperature of the MgO was assumed to be equal to the temperature inferred using pyrometry, that is, the temperature of the Mg-MgO interface. Axial temperature gradients were clearly present in the MgO, with the MgO in contact with the diamond anvil being significantly cooler than that in contact with the sample. A temperature difference of 1000 K corresponds to a pressure difference of approximately 7 GPa.<sup>32</sup> Upon heating, the integrated diffraction peaks from the MgO were noticeably broader than those from the sample. The additional width of the MgO peaks suggests a temperature gradient of around 500 K at a sample temperature of 1000 K, rising to around 700 K at a sample temperature of 2500 K. The stated pressures may thus be systematically 3-6 GPa too high, with the higher discrepancies at the higher temperature and higher pressure region of the phase diagram.

## EXPERIMENTAL RESULTS

### Room Temperature Compression and Equation of State

In addition to the DAC specifically prepared to measure the RT compression beyond 200 GPa (cell 1), one of the gas-membrane DACs used for resistive heating (henceforth labeled cell 2) was first pressurised at RT to 78.1 GPa, before being decompressed to 32.7 GPa, in order to study the bcc-to-hcp transition on both compression and decompression. As mentioned previously, neither cell 1 or 2 contained any pressure transmitting medium, and both contained a Cu pressure marker.

On pressure increase in cell 2, diffraction peaks from the bcc phase were first observed at 46(2) GPa, at the lower end of the transition pressure range of 50(6) GPa reported by Olijnyk and Holzapfel.<sup>11</sup> On further pressure increase we observed a large region of phase co-existence of the bcc and hcp phases, as previously reported,<sup>11</sup> such that the hcp phase was absent only above 61(1) GPa. In cell 1, we observed a considerably smaller co-existence

region, with the bcc phase emerging at 50(2) GPa and single-phase patterns were observed above 58(2) GPa. On decompression of cell 2 from 78 GPa, the reverse bcc-to-hcp transition was found to start at 44.9(13) GPa and single-phase profiles of the hcp phase were observed only below 36(1) GPa.

After obtaining single-phase profiles of the bcc phase, the sample pressure in cell 1 was increased to a maximum pressure of 211 GPa. No further phase transitions were observed, and the bcc phase was found to be stable at RT to this maximum pressure. The RT compressibility of the hcp and bcc phases on both pressure increase and decrease, as obtained from the samples in cells 1 and 2, is shown in Figure 1. From mixed-phase profiles obtained between 47 and 57 GPa, the volume change ( $\Delta V/V_0$ ) at the hcp-to-bcc transition is determined to be 0.45(18)% (see inset to Figure 1), in excellent agreement with the volume difference of 0.4(4)% reported by Nishimura *et al.*<sup>10</sup>

The compressibilities of the hcp and bcc phases were fitted with two separate Vinet<sup>33</sup> equations of state (EoS) using the EOSFIT package.<sup>34</sup> For comparison with previous studies,<sup>7,10,19</sup> the same data were also fitted with a Birch-Murnaghan (B-M) EoS.  $V_0$  of the hcp phase was fixed at its experimentally-determined value of 23.1495(8) Å<sup>3</sup> per atom. Determining the value of  $V_0$  for the high-pressure bcc phase presented a greater problem, as this phase is not stable at ambient pressure, and refining a value for  $V_0$  within EOSFIT showed that this parameter was correlated with both  $K_0$  and  $K'$  at more than 98%. Liu *et al.*<sup>7</sup> calculated the relative volumes of the hcp and bcc phases at ambient pressure (at 0 K), and determined that the atomic volume of the bcc phase was 0.043% smaller than that of the hcp phase. This implies a value of  $V_0$  for the bcc phase of 23.1398(8) Å<sup>3</sup> per atom, and  $K_0$  and  $K'$  for the bcc phase were therefore refined with  $V_0$  fixed at this value. The results of all of the EoS fits are shown in Table I. The bulk modulus determined here for the hcp phase using a Vinet EoS is smaller than those determined previously,<sup>7,10,19</sup> although use of the B-M EoS gives slightly better agreement.

The EoS values determined for the bcc phase with a fixed  $V_0$  are reasonably similar to those of Liu *et al.*<sup>7</sup>, but disagree with the values of Nishimura *et al.*<sup>10</sup>. However, the value Nishimura *et al.* determine for  $V_0$  of the bcc phase is very small compared to that of the hcp phase. Allowing  $V_0$  to refine, and using a B-M EoS, gave values for  $K_0$  and  $K'$  of 45(8) GPa and 3.8(1), respectively, much closer to those of Nishimura *et al.* - see Table I. However, the large correlation between all parameters in this fit, together with the small value of  $V_0$

(21.7(9) Å<sup>3</sup> per atom) and the large uncertainties in the values, means we do not place much faith in the results obtained from these non-constrained fits for the bcc phase, nor those of Nishimura *et al.*

## RESISTIVE HEATING STUDIES

The DACs used for the resistive heating studies were all initially pressurised to approximately 20 GPa, and then heated to 780, 700, 630, 480 and 400 K, with the sixth cell being compressed at RT for comparison. The diffraction data obtained on compression and decompression at 700 K are shown in Figure 2, and the results obtained at the six different temperatures are summarised in Figure 3.

A number of conclusions can be drawn from these measurements. Firstly, the pressure at which the bcc phase first appears on compression increases slightly with increasing temperature, from 46.1(8) GPa at 400 K to 46.8(6) GPa at 700 K. However, the pressure at which the phase transition to the bcc was completed demonstrates a more dramatic change, dropping from ~61 GPa between 300 and 480 K to 55(2) GPa at 700 K. Unfortunately, due to a sudden jump in pressure, it was not possible to obtain accurate transition pressures on compression from the sample at 780 K. However, a single-phase bcc pattern was obtained at 52.0(3) GPa at 780 K, demonstrating a further drop in the transition completion pressure with temperature increase above 700 K. This decrease in the size of the mixed-phase region with temperature is to be expected, as it becomes easier to overcome the kinetic barriers to reach whichever phase is more thermodynamically stable.

Problems with seizure of the piston-cylinders in the DACs on pressure decrease at high temperatures meant that sufficient measurements to determine the transition region on decompression were obtained at only three temperatures, 300 K, 700 K and 780 K. The mixed-phase region on decompression both decreases in pressure, and becomes narrower, with increasing temperature, from between 44.9(15) GPa and 36.0(9) GPa at 300 K to between 40.3(3) GPa and 33.9(5) GPa at 780 K. The general decrease in transition pressure with temperature agrees with calculations of Moriarty and Althoff,<sup>4</sup> and also Mehta *et al.*,<sup>6</sup> both of whom predicted the hcp-bcc phase line to have a negative slope. The slope calculated by Moriarty and Althoff is more negative than we observe, while the phase transition line calculated by Mehta *et al.* below 800 K lies within the mixed-phase region determined here.

## LASER HEATING STUDIES

The 12 Boehler-Almax Plate DACs prepared for laser heating, as described above, were precompressed to a range of pressures between 5.7 GPa and 90 GPa prior to heating. For each pressure cell, diffraction patterns were initially collected continuously as the powers of the two lasers were ramped manually from 0.3 W to 62 W, with the powers of the two lasers illuminating each side of the sample adjusted to minimize temperature differences. However, it was noticed that sometimes the intensity of the thermal radiation decreased with time at constant laser power. In these cases, we switched to short pulse (a few seconds) heating, and x-ray diffraction patterns were collected only during this short period. The exposure times for the diffraction patterns for each cell were therefore different, and varied from less than 1 s to 10 s. For all samples, the laser power was increased until either the sample melted, as described below, or the onset of large fluctuations in the thermal radiation emitted from the sample precluded further temperature measurements *via* spectroradiometry. The onset of these rapid fluctuations was accompanied by recrystallisation of the sample, as judged by the changes in the positions of Bragg peaks on the detector from exposure to exposure. This phenomenon appears to be similar to that observed by Lazicki *et al.* in their recent laser-heating studies of Be.<sup>35</sup>

Detecting the existence of molten Mg, and determining the temperature at which melting occurs, is challenging. It is generally accepted that the complete disappearance of crystalline Bragg scattering is an indicator of melting. While this is necessary, however, it is not sufficient, and the observation of a diffuse halo of scattering from the liquid is also required for definitive proof of melting. But, for weakly scattering samples such as Li<sup>36</sup> and Be,<sup>35</sup> diffuse scattering from the liquid has not been observed, even in relatively large, resistively-heated samples. In the current study, we were able to observe the disappearance of all Bragg scattering from the crystalline phases at clearly discernible temperatures, which we have interpreted as the melting temperature. However, above the melting temperature we were not able to obtain any measurable scattering from the liquid phase. In addition to the disappearance of all Bragg scattering, in many samples we were also able to observe the onset of rapid recrystallisation of the samples at clearly defined temperatures below that of the melting temperature. Similar behaviour has recently been reported in laser-heating diffraction studies of Be,<sup>35</sup> Mo<sup>37</sup> and Fe.<sup>38</sup> This recrystallisation behavior was clearly distin-

guishable from the disappearance of the Bragg scattering at higher temperatures that we associated with melting. In some of the samples, the rapid-recrystallisation of the sample also produced rapid and very large fluctuations in the measured temperature, which precluded further studies at higher temperatures, and thus the determination of true melting in these samples.

The ADXRD patterns collected from the laser-heated samples revealed the clear existence of only the hcp and bcc phases below the melting curve, with some evidence of a third phase in the vicinity of 5 GPa and 1200 K, which is shown in Figure 4. This is the same region of the phase diagram in which Errandonea *et al.*<sup>19</sup> reported the existence of the dhcp phase. While the diffraction patterns obtained near 6 GPa and 1200 K contain some of the features expected from the dhcp structure, there are also two additional diffraction peaks at  $d$ -spacings of 2.24 Å and 1.40 Å, which are explained by neither the hcp or dhcp phase. These two peaks were not observed by Errandonea *et al.*<sup>19</sup> All of the additional peaks were still observed after the sample was cooled to RT, as observed previously by Errandonea *et al.*<sup>19</sup>, and analysis of their positions and relative intensities showed that they do not arise from the formation of the Cu-Mg alloys Cu<sub>2</sub>Mg or Mg<sub>2</sub>Cu, assuming that the crystal structures of these alloys at 5-6 GPa is the same as that at ambient pressure. Attempts to index all of the observed diffraction peaks as coming from a single phase were also unsuccessful, and we cannot therefore make any definitive statement on the existence, or otherwise, of the dhcp phase. Only the lowest-pressure of our twelve samples showed any evidence of this phase, and further detailed investigations of this region of the phase diagram are required.

As observed both at RT and in the resistive-heating studies, mixed-phase diffraction profiles containing both the hcp and bcc phases were found across a wide region of  $P$ - $T$  space during the laser-heating studies. The pressure at which the bcc phase is first observed continues to decrease with increasing temperature, reaching 36 GPa at 1630 K. The bcc-hcp phase line is thus more vertical at higher temperatures than those calculated by Moriaty and Althoff,<sup>4</sup> and Mehta *et al.*,<sup>6</sup> and we can estimate that the hcp-bcc-liquid triple point is around 25 GPa and 2100 K. All of the present results are combined with previous studies of transitions and melting of Mg into the comprehensive phase diagram of Mg to 105 GPa shown in Figure 5.

The bcc phase was clearly observed at both 89 GPa & 3980 K and 97 GPa & 4320 K, above the melting line of Errandonea *et al.*<sup>16</sup> A modification to the melting curve to account

for these points is given in Figure 5. There are two possible reasons for the discrepancy in the two data sets. Firstly, Errandonea *et al.* detected melting using the speckle method, where the onset of melting is detected by observing movement at the Mg surface. Detecting this movement becomes more difficult as pressure increases (among other things because the viscosity of the liquid increases). Also recrystallisation may occur at temperatures significantly below the melting temperature, leading to movement that is similar to the motion from melting. As a consequence of this, the melting temperature may have been underestimated beyond 60 GPa. Secondly, in laser heating there are axial temperature gradients in the sample, even when using double-sided heating. The center of the sample will therefore be cooler than the surface, and the temperature is measured from the surface. It is thus possible that even after the onset of melting at the surface, the centre of the sample is still a solid and still diffracting. It should be noted that the disagreement with the data of Errandonea *et al.* is primarily due to a single point in their work at 87 GPa and 3480 K. The upper part of the error bars of the rest of the data gives reasonable agreement with the lowest part of the current data.

## CONCLUSIONS

The phase diagram of magnesium has been extended to 211 GPa at room temperature, and to 105 GPa at 4500 K. At 300 K, the onset of the hcp to bcc phase transition is observed at 46-50 GPa, probably dependent on how hydrostatic the sample in each cell is. The bcc phase was found to be stable to 211 GPa. The extended pressure range of our measurements, and the correction of our data for the effects of non-hydrostatic pressures, has enabled us to determine a more accurate EoS for the bcc phase. From our resistive heating studies, the slope of the hcp-bcc phase boundary has been determined experimentally for the first time, and is of the order of -130 K/GPa. While the negative slope is in agreement with the theoretical predictions of Moriarty and Althoff, and Mehta *et al.*,<sup>4,6</sup> the experimental phase boundary is noticeably more vertical than the results of the calculations above 800 K.

Our new melting temperature data to 100 GPa do not reproduce the previously-reported sharp change in the slope of the melting curve around 50 GPa. Rather, we observe only a slight change in the slope with pressure, such that at 100 GPa the melting temperature is 4300 K, some 800 K higher than previously reported. This difference in temperature

probably results from the different methods used to detect the onset of melting.

Finally, the additional diffraction peaks reported by Errandonea *et al.*<sup>19</sup> in the vicinity of 10 GPa and 1300 K are also observed in the current study, and, as in that study, these peaks are found to remain on cooling back to room temperature. However, we cannot assign all of the peaks to the dhcp structure suggested by Errandonea *et al.*<sup>19</sup> The origin of these peaks, and whether they come from a further phase of Mg, is therefore still unknown and a further detailed study of the Mg phase diagram in the region of 10 GPa and 1300 K is still required.

## ACKNOWLEDGEMENTS

Portions of this work were performed at HPCAT (Sector 16), Advanced Photon Source (APS), Argonne National Laboratory. HPCAT operations are supported by DOE-NNSA under Award No. DE-NA0001974 and DOE-BES under Award No. DE-FG02-99ER45775, with partial instrumentation funding by NSF. APS is supported by DOE-BES, under Contract No. DE-AC02-06CH11357. This work was performed under the auspices of the U.S. Department of Energy by Lawrence Livermore National Laboratory in part under Contract W-7405-Eng-48 and in part under Contract DE-AC52-07NA27344. ©British Crown Owned Copyright 2014/AWE. Published with permission of the Controller of Her Britannic Majesty's Stationery Office. MIM is grateful to AWE Aldermaston for the award of a William Penney Fellowship. DE thanks the financial support of the Spanish MINECO under Grants No. MAT2010-21270-C04-01 and No. CSD2007-00045. We would like to thank Heribert Wilhelm and Annette Kleppe at I15 at the Diamond Light Source for their support.

---

<sup>1</sup> A. K. McMahan, *Physica B & C* **139**, 31 (1986).

<sup>2</sup> J. D. Althoff, P. B. Allen, R. M. Wentzcovitch, and J. A. Moriarty, *Physical Review B* **48**, 13253 (1993).

<sup>3</sup> R. Ahuja, O. Eriksson, J. M. Wills, and B. Johansson, *Physical Review Letters* **75**, 3473 (1995).

<sup>4</sup> J. A. Moriarty and J. D. Althoff, *Physical Review B* **51**, 5609 (1995).

<sup>5</sup> G. R. Chavarria, *Physics Letters A* **336**, 210 (2005).

<sup>6</sup> S. Mehta, G. D. Price, and D. Alfè, *The Journal of Chemical Physics* **125**, 194507 (2006).

- <sup>7</sup> Q. Liu, C. Fan, and R. Zhang, *Journal of Applied Physics* **105**, 123505 (2009).
- <sup>8</sup> C. J. Pickard and R. J. Needs, *Nature Materials* **9**, 624 (2010).
- <sup>9</sup> Y. Yao and D. D. Klug, *Journal of Physics-Condensed Matter* **24**, 265401 (2012).
- <sup>10</sup> N. Nishimura, K. Kinoshita, Y. Akahama, and H. Kawamura, in *Proc. The 20th AIRAPT Int. Conf. on High Pressure Science and Technology* (Mineralogical Soc. America, Karlsruhe, Germany, 2005), pp. T10–P054.
- <sup>11</sup> H. Olijnyk and W. B. Holzapfel, *Physical Review B* **31**, 4682 (1985).
- <sup>12</sup> A. K. McMahan and J. A. Moriarty, *Physical Review B* **27**, 3235 (1983).
- <sup>13</sup> P. Li, G. Gao, Y. Wang, and Y. Ma, *Journal of Physical Chemistry C* **114**, 21745 (2010).
- <sup>14</sup> G. C. Kennedy and R. C. Newton, *Solids Under Pressure* (McGraw-Hill, New York, USA, 1963).
- <sup>15</sup> D. Errandonea, *Journal of Applied Physics* **108**, 033517 (2010).
- <sup>16</sup> D. Errandonea, R. Boehler, and M. Ross, *Physical Review B* **65**, 012108 (2001).
- <sup>17</sup> There is a typographical error in Ref. 16, where the gradient of the melting curve is stated to be 6 K/GPa. The true value of 45 K/GPa is clear from Fig. 1 of Ref 16.
- <sup>18</sup> D. Milathianaki, D. C. Swift, J. Hawreliak, B. S. El-Dasher, J. M. McNaney, H. E. Lorenzana, and T. Ditmire, *Physical Review B* **86**, 014101 (2012).
- <sup>19</sup> D. Errandonea, Y. Meng, D. Häusermann, and T. Uchida, *Journal of Physics-Condensed Matter* **15**, 1277 (2003).
- <sup>20</sup> H. Cynn, W. Evans, C. S. Yoo, Y. Ohishi, N. Sata, and O. Shimomura, in APS March Meeting, 22-26 March 2004, Sec. W20.009. (2004).
- <sup>21</sup> R. Boehler and K. De Hantsetters, *High Pressure Research* **24**, 391 (2004).
- <sup>22</sup> Z. Jenei, H. Cynn, K. Visbeck, and W. J. Evans, *Review of Scientific Instruments* **84**, 095114 (2013).
- <sup>23</sup> G. Y. Shen, M. L. Rivers, Y. B. Wang, and S. R. Sutton, *Review of Scientific Instruments* **72**, 1273 (2001).
- <sup>24</sup> R. Boehler, H. G. Musshoff, R. Ditz, G. Aquilanti, and A. Trapananti, *Review of Scientific Instruments* **80**, 045103 (2009).
- <sup>25</sup> A. P. Hammersley, S. O. Svensson, M. Hanfland, A. N. Fitch, and D. Häusermann, *High Pressure Research* **14**, 235 (1996).
- <sup>26</sup> A. Le Bail, H. Duroy, and J. L. Fourquet, *Materials Research Bulletin* **23**, 447 (1988).
- <sup>27</sup> A. A. Coelho, *Topas Academic* (2007).

- <sup>28</sup> H. Cynn, *Unpublished*.
- <sup>29</sup> A. K. Singh and K. Takemura, *Journal of Applied Physics* **90**, 3269 (2001).
- <sup>30</sup> K. Takemura and A. K. Singh, *Physical Review B* **73**, 224119 (2006).
- <sup>31</sup> S. Speziale, C.-S. Zha, T. S. Duffy, R. J. Hemley, and H.-K. Mao, *Journal of Geophysical Research: Solid Earth* **106**, 515 (2001), ISSN 2156-2202.
- <sup>32</sup> Y. Tange, Y. Nishihara, and T. Tsuchiya, *J. Geophys. Res.* **114**, B03208 (2009).
- <sup>33</sup> P. Vinet, J. Ferrante, J. H. Rose, and J. R. Smith, *Journal of Geophysical Research: Solid Earth* **92**, 9319 (1987).
- <sup>34</sup> R. Angel, in *High-Temperature and High-Pressure Crystal Chemistry* (Mineralogical Soc America, 2000), vol. 41 of *Reviews In Mineralogy & Geochemistry*, pp. 35–59.
- <sup>35</sup> A. Lazicki, A. Dewaele, P. Loubeyre, and M. Mezouar, *Physical Review B* **86**, 174118 (2012).
- <sup>36</sup> C. L. Guillaume, E. Gregoryanz, O. Degtyareva, M. I. McMahon, M. Hanfland, S. Evans, M. Guthrie, S. V. Sinogeikin, and H.-K. Mao, *Nature Physics* **7**, 211 (2011).
- <sup>37</sup> D. Santamaría-Pérez, M. Ross, D. Errandonea, G. D. Mukherjee, M. Mezouar, and R. Boehler, *Journal of Chemical Physics* **130**, 124509 (2009).
- <sup>38</sup> S. Anzellini, A. Dewaele, M. Mezouar, P. Loubeyre, and G. Morard, *Science* **340**, 464 (2013).
- <sup>39</sup> P. A. Urtiew and R. Grover, *Journal of Applied Physics* **48**, 1122 (1977).
- <sup>40</sup> L. J. Slutsky and C. W. Garland, *Physical Review* **107**, 972 (1957).

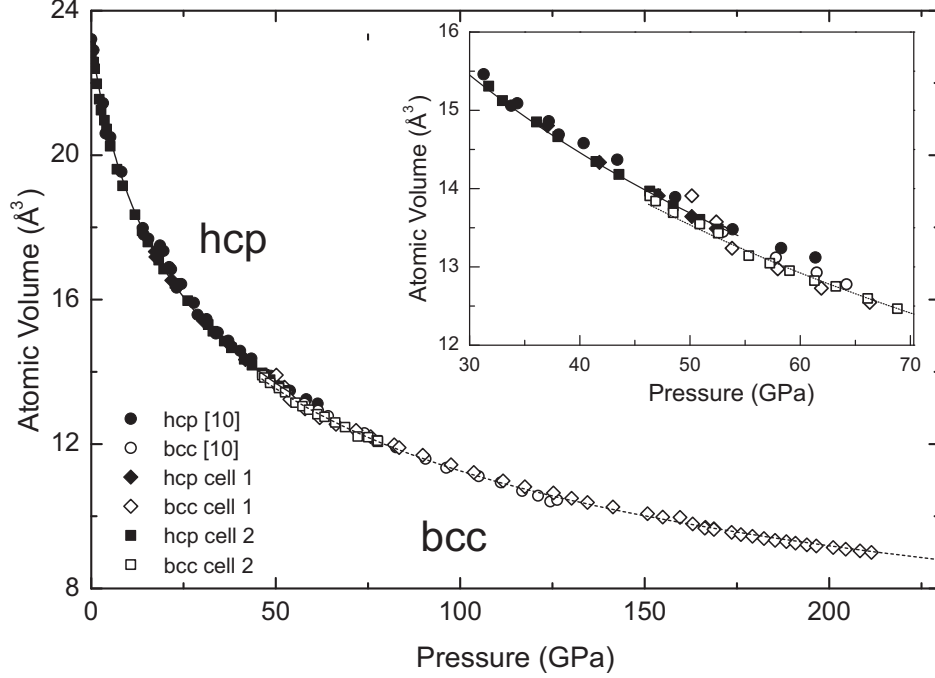


FIG. 1. The atomic volume of Mg as a function of pressure to 211 GPa at 300 K, as obtained from cells 1 and 2 (see main text for descriptions of each). Data points from the hcp phase are shown using solid symbols, while data from the bcc phase are shown using open symbols. Data from cells 1 and 2 are plotted using diamonds and squares, respectively. The data of Nishimura *et al.*,<sup>10</sup> plotted with filled and open circles, are shown for comparison. The solid and dashed lines show the Vinet equations-of-state for the hcp and bcc phases, as determined from the current data, using the parameters given in Table I. All error bars are smaller than the symbols used to plot the data. The inset shows an enlarged view of the atomic volume at pressures between 30 and 70 GPa, and highlights the volume change at the hcp-to-bcc transition.

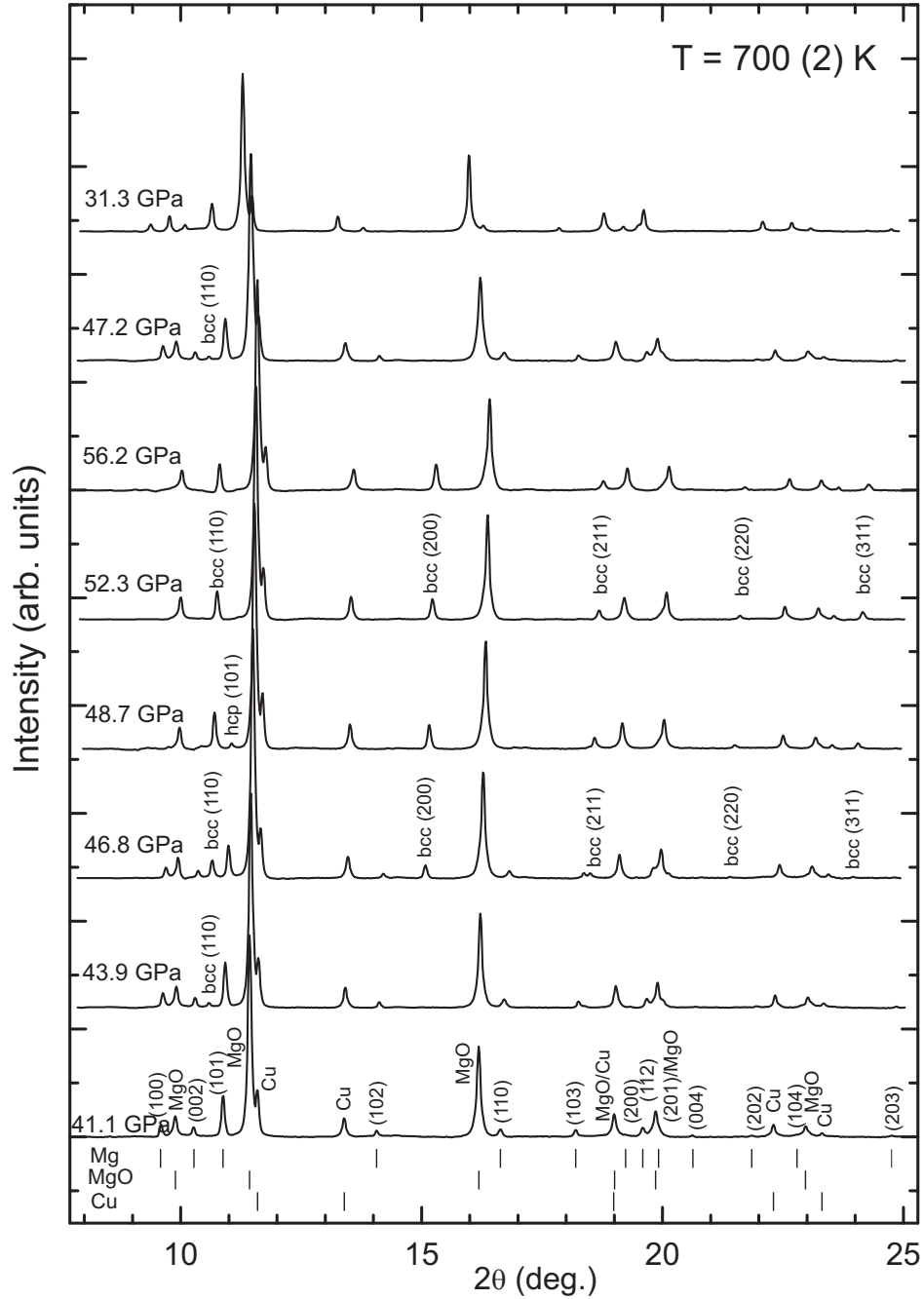


FIG. 2. Diffraction profiles collected on pressure increase from 41.1 to 56.2 GPa, and then back down to 31.3 GPa, at 700 K. The diffraction peaks from the Mg sample, MgO PTM and Cu pressure marker are identified with tickmarks beneath the bottom profile. Indices are given for the most intense diffraction peaks from each of the three materials. All diffraction patterns have had a smoothly varying background removed for clarity.

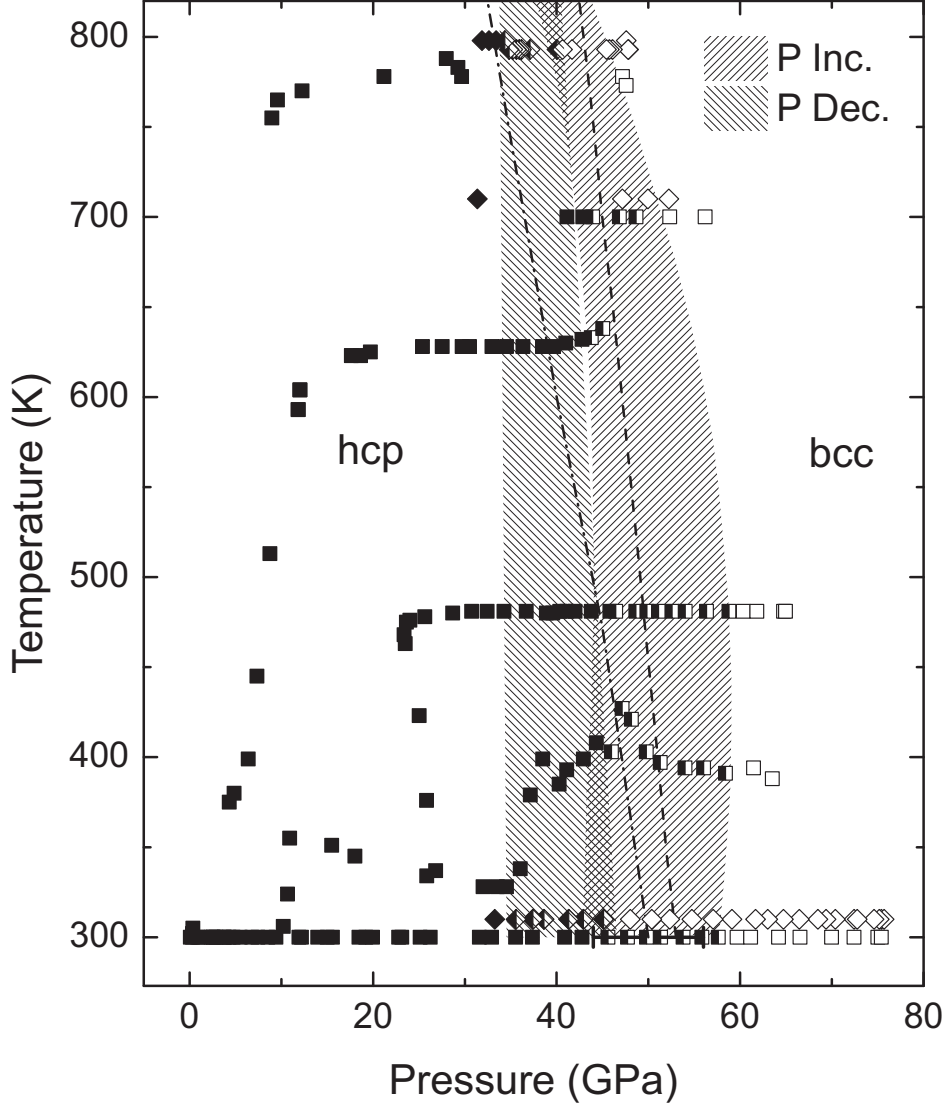


FIG. 3. The temperature dependence of the hcp-to-bcc phase transition pressure in Mg on compression. The  $P$ - $T$  conditions at which single-phase hcp, mixed-phase hcp-bcc, and single-phase bcc profiles are observed are shown using filled, half-filled, and unfilled symbols, respectively. Data collected on pressure increase are plotted with squares, while data collected on pressure decrease are plotted using diamonds. The data collected on pressure decrease have been offset vertically by +10 K (at 300 K and 700 K) and +15 K (at 780 K) for clarity. The dot-dashed and dashed lines highlight the phase boundaries calculated by Moriarty and Althoff<sup>4</sup> and Mehta *et al.*<sup>6</sup>, respectively. The two hatched areas shows the mixed-phase regions determined in the current study on pressure increase and decrease.

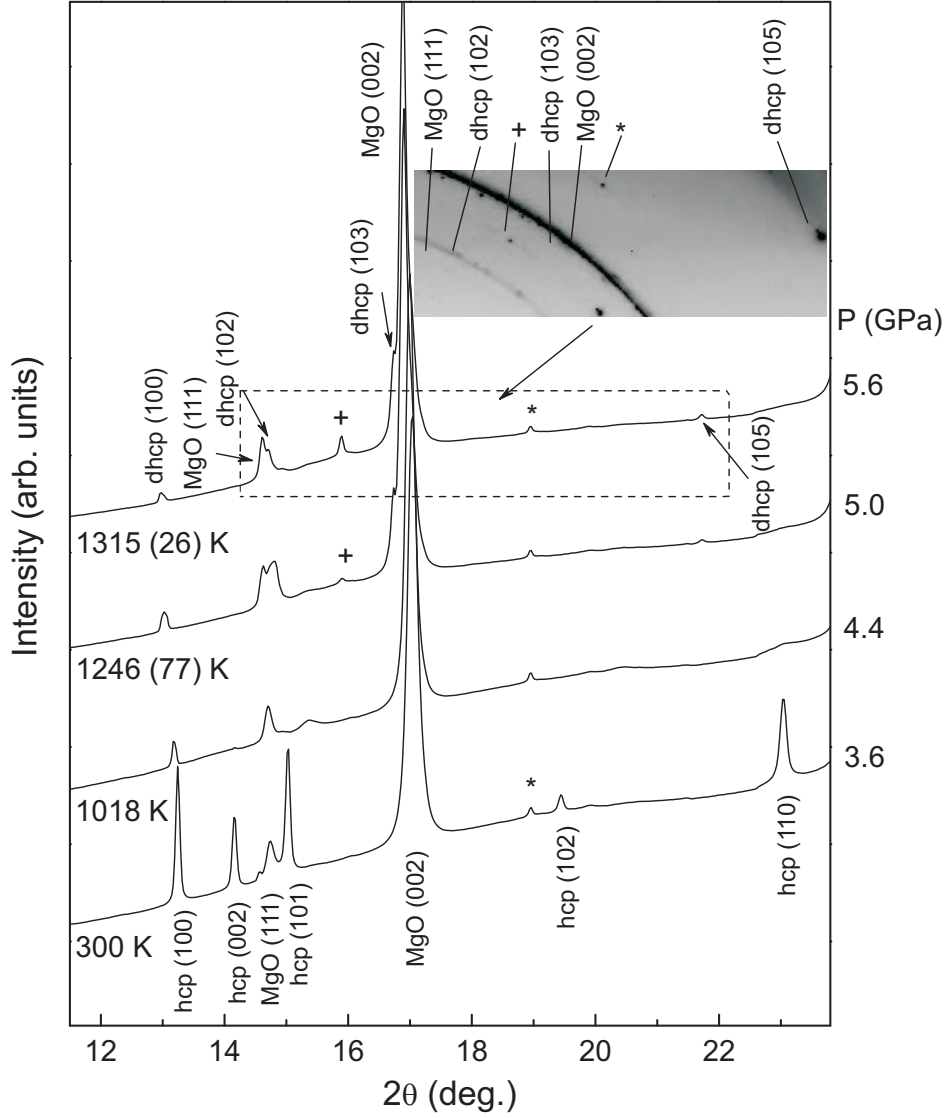


FIG. 4. Integrated diffraction patterns obtained on laser heating Mg from 300 K to 1315 K at 3.6 to 5.6 GPa. Two diffraction peaks, which can be indexed as the (103) and (105) peaks from a dhcp structure, appear at 1246(77) K, and are indexed in the highest-temperature profile. Two additional reflections, not fitted by the dhcp structure, appear at  $15.9^\circ$  ( $2.24 \text{ \AA}$ ) and  $25.6^\circ$  ( $1.40 \text{ \AA}$ ), and the lowest-angle of the two peaks is highlighted with a + symbol. The inset shows part of the 2D diffraction image collected at 1315 K, illustrating the spotty texture of the sample peaks.

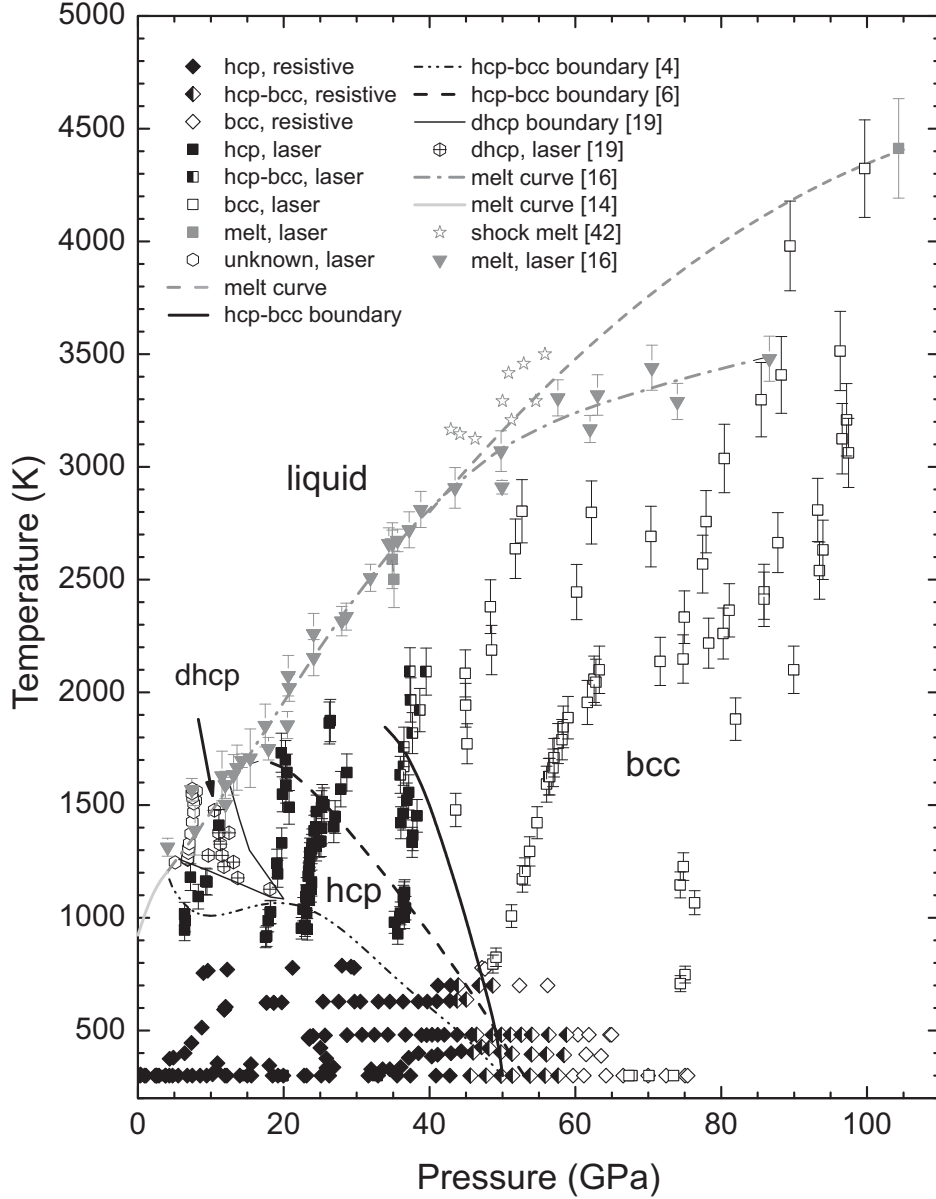


FIG. 5. The  $P$ - $T$  phase diagram of Mg to 105 GPa and 4500 K. hcp-phase points are shown in black, bcc-phase points are shown using unfilled symbols and mixed-phase points are shown using half-filled symbols. Points where melting is observed are plotted with grey-filled symbols. Data plotted with square symbols are from the laser-heating portion of this study, and diamond symbols plot the resistive heating data. The circular symbols with crosses around 15 GPa and 1300 K are those labeled dhcp in Errandonea *et al.*,<sup>19</sup>; points where extra diffraction peaks were observed in this study are shown as open circles. The data plotted with stars near 50 GPa and 3500 K show the melt points from Urtiew and Grover.<sup>39</sup> Grey, downward-pointing triangles show the melting points from Errandonea *et al.*,<sup>16</sup> with the grey dot-dash line showing the fit to these data from the same work. The grey dashed line at higher temperature is an extension to the Errandonea *et al.* melt line above 50 GPa, extrapolated to give the best agreement with the present data. The black lines at lower pressures show the hcp-bcc phase boundaries of Moriarty and Althoff<sup>4</sup> (dotted) and

TABLE I. Results of fitting the experimental volumes of the hcp and bcc phases with Vinet and Birch-Murnaghan (B-M) equations of state, with the most recently published experimental and theoretical values for comparison. The bulk modulus of Slutsky and Garland<sup>40</sup> is the adiabatic value calculated from the measured elastic constants.

hcp						
	This Study	This Study	Nishimura <i>et al.</i> <sup>10</sup>	Errandonea <i>et al.</i> <sup>19</sup>	Liu <i>et al.</i> <sup>7</sup>	Slutsky and Garland <sup>40</sup>
	X-ray Diffraction	X-ray Diffraction	X-ray Diffraction	X-ray Diffraction	DFT	Ultrasound
EoS	Vinet	B-M	B-M	B-M	B-M	
$V_0$ ( $\text{\AA}^3$ )	23.1495(fixed)	23.1495 (fixed)	23.222(2)	23.05(15)	23.027	
$K_0$ (GPa)	30.9(4)	32.5(4)	36.7(17)	36.8(30)	36.038	35.24
$K'$	4.56(6)	4.05(5)	3.7(4)	4.3(4)	3.831	
bcc						
	This Study	This Study	Nishimura <i>et al.</i> <sup>10</sup>	Liu <i>et al.</i> <sup>7</sup>		
	X-ray Diffraction	X-ray Diffraction	X-ray Diffraction	DFT		
EoS	Vinet	B-M	B-M	B-M		
$V_0$ ( $\text{\AA}^3$ )	23.1394 (fixed)	21.7(9)	19.95(7)	23.017		
$K_0$ (GPa)	26.3 (6)	45(8)	68.7(7)	35.997		
$K'$	5.10(6)	3.8(1)	3.47(4)	3.817		